Received: 21 March 2020 | Revised: 6 June 2020 | Accepted: 9 June 2020
DOI: 10.1002/aoc.5916

FULL PAPER

Applied Organometallic Chemistry WILEY

Synthesis and characterization of mesoporous organosilica supported palladium (SBA-Pr-NCQ-Pd) as an efficient nanocatalyst in the Mizoroki–Heck coupling reaction

Razieh Moradi[1] | **Ghodsi Mohammadi Ziarani**[1] | **Alireza Badiei**[2] | **Fatemeh Mohajer**[1]

[1]Department of Chemistry, Alzahra University, Vanak Square, Tehran, Iran
[2]School of Chemistry, College of Science, University of Tehran, Tehran, Iran

Correspondence
Ghodsi Mohammadi Ziarani, Department of Chemistry, Alzahra University, Vanak Square, Tehran, Iran, P.O. Box 1993893973.
Email: gmohammadi@alzahra.ac.ir; gmziarani@hotmail.com

In the present study, the modification of a mesoporous organosilica nanocomposite SBA-15 (Santa Barbara Amorphous 15) was carried out in two steps, first through the surface functionalization of SBA-Pr-NH_2 with 2-chloroquinoline-3-carbaldehyde to form SBA-Pr-NCQ, and then through a post-modification process with palladium ions. The target nanocompound structure of SBA-Pr-NCQ-Pd was characterized by different techniques (thermogravimetric analysis, X-ray diffraction, scanning electron microscopy, Energy-dispersive X-ray spectroscopy (EDX), and Fourier transform infrared spectroscopy). The catalytic performance of the porous inorganic–organic hybrid nanocomposite (SBA-Pr-NCQ-Pd) in one of the most important carbon–carbon bond-forming processes, the Mizoroki–Heck coupling reaction of aryl halides and methacrylate in water/ethanol media, was examined. Compared to previous reports, this protocol afforded some advantages, such as high yields of products, short reaction times, catalyst stability without leaching, simple methodology, easy workup, and greener conditions. Also, the nanocatalyst can be easily separated from the reaction mixture and reused several times without a significant decrease in activity and promises economic as well as environmental benefits.

KEYWORDS
2-chloroquinoline-3-carbaldehyde, functionalization, SBA-Pr-NCQ, SBA-Pr-NCQ-Pd, Mizoroki-Heck coupling reaction reaction

1 | INTRODUCTION

Nanoreactors are effective catalytic systems that have a porous structure and dimensions smaller than 100 nm. They not only provide an atmosphere conducive to interaction between molecules but also control and accelerate the reaction. Various kinds of nanoreactors have been established, including zeolites,[1] metal–organic frameworks,[2] carbon nanotubes,[3] dendrimers,[4] and mesoporous silicas.[5] Recently, mesoporous materials, especially SBA-15, have been extensively studied.[6–9] These materials, with surface chemistry and controllable pore structure, have attracted considerable attention from academia and industry. In particular, mesoporous silicas are of great importance for the fabrication of inorganic–organic

https://doi.org/10.1002/aoc.5916

hybrid materials due to their highly desirable properties, such as pore topologies that possess long-range structural ordering, uniform pore sizes in the 2–10 nm range, and highly specific surface areas, which can be easily functionalized.[10–15] So, these materials which are obtained by surfactant-directed self-assembly of various organosilane precursors, display great potential for high-performance catalysts with desired catalytic activity and extend lifetime.[16,17]

On the other hand, the Heck reaction, the palladium-catalyzed coupling of olefins with aryl or vinyl halides, is one of the strategies to form a new carbon–carbon (Csp^2–Csp^2) bond in synthesis. Since the discovery of this reaction by Heck and Mizoroki et al.,[18,19] it has been widely studied[20,21] and applied to various fields, such as the synthesis of natural products,[22] material science,[23] and bioorganic chemistry.[24] A major transformation in the Heck reaction is the synthesis of cinnamic acid and its derivatives, which are important intermediates in the synthesis of medical products and are frequently used as UV absorbents and flavor substances.[25] The reaction is commonly catalyzed by palladium complexes in a homogeneous operation mode and shares general drawbacks, that is, catalyst recovery and recycling are hard. Furthermore, expensive, generally unstable, and toxic ligands, such as phosphine, need to activate and stabilize Pd against agglomeration and generation of Pd black.[26] Thus, inexpensive and environmentally friendly heterogeneous catalysts are interesting and important. Palladium supported on a variety of organic and inorganic materials, such as carbon,[27] metal oxides,[28] clay,[29] polymers,[30] ordered[31] or amorphous silicates[32], and zeolites,[33] were established and applied as a catalyst in the Heck reaction. Among them, palladium nanoparticles (Pd NPs) supported on the hexagonal structure of SBA-15 can be evenly dispersed, thus efficiently preventing Pd NP aggregation.[34,35] To develop the applicability as well as the stability of Pd-decorated SBA-15 materials in air and aqueous media, the surface has to be improved using organic functional groups by appropriate organic ligands as linkers between SBA-15 silica and Pd.[36] Recently, various types of Pd-anchored ligand-based SBA-15 have been reported as the catalyst in the Heck reaction.[37–44] However, to improve these advantages, and in continuation of our recent study of the field of mesoporous organosilica nanoreactors[45] and the importance of palladium-catalyzed coupling reactions as a powerful toolbox in the synthetic organic chemistry, we report the preparation and characterization of a novel mesoporous organosilica supported palladium nanoparticle, SBA-Pr-NQC-Pd, as well as its catalytic application in the Mizoroki–Heck coupling reaction of aryl halides with methacrylate.

2 | EXPERIMENTAL

General method, instrument, and synthesis of SBA-15, SBA-Pr-NH_2 and 2-chloroquinoline-3-carbaldehyde are presented in the supporting information. The FT-IR, TGA, and SEM of SBA-Pr-NH_2 are also given in supporting information (Figures S1-S3).

2.1 | Synthesis of SBA-Pr-NCQ

First, 2-chloroquinoline-3-carbaldehyde (0.95 g 5 mmol) was added to the dispersed SBA-Pr-NH_2 (1 g) in ethanol and refluxed for 48 hr. The obtained yellow powder was then filtered and washed with an excess of toluene and any residual organosilane was removed by Soxhlet extraction in ethanol over a 24-hr period. The final product was obtained as a yellow powder after washing with an excess of ethanol and drying at ambient temperature. The IR and EDX of SBA-Pr-NCQ are provided in supporting information (Figure S4 and S5).

2.2 | Immobilization of Pd(II) ions on the surface of SBA-Pr-NCQ

A mixture of SBA-Pr-NCQ (1.0 g) and palladium chloride (0.177 g, 1 mmol) in ethanol (30 ml) was refluxed for 48 hr, and the dark green obtained solid was filtered, washed with acetone, and dried in vacuum at 80°C for 2 hr to give SBA-Pr-NCQ-Pd(II).

2.3 | Mizoroki–Heck coupling reaction

In general, a mixture of aryl halide (1 mmol), methacrylate (103 ml, 1.2 mmol), potassium carbonate (276.4 g, 2 mmol), SBA-Pr-NCQ-Pd (0.25 mol%), and a mixture of ethanol and water (2:3, 5 ml) was placed in a 25-ml round-bottomed flask and heated for the desired time (as shown in Table 2) at 70°C. The reaction completion was monitored by thin-layer chromatography (hexane: ethyl acetate, 4:1). After cooling the reaction mixture to room temperature, the catalyst was recovered by filtration and washed with ethyl acetate and ethanol. The organic layer was separated and dried over anhydrous calcium chloride to afford the desired products.

3 | RESULTS AND DISCUSSION

3.1 | Catalyst characterization

The synthesis of SBA-Pr-NCQ-Pd is shown in Scheme **1**. In the first step, the Vilsmeier–Haack[46] reaction of DMF **1** and $POCl_3$ **2** formed intermediate **3**, which reacted with

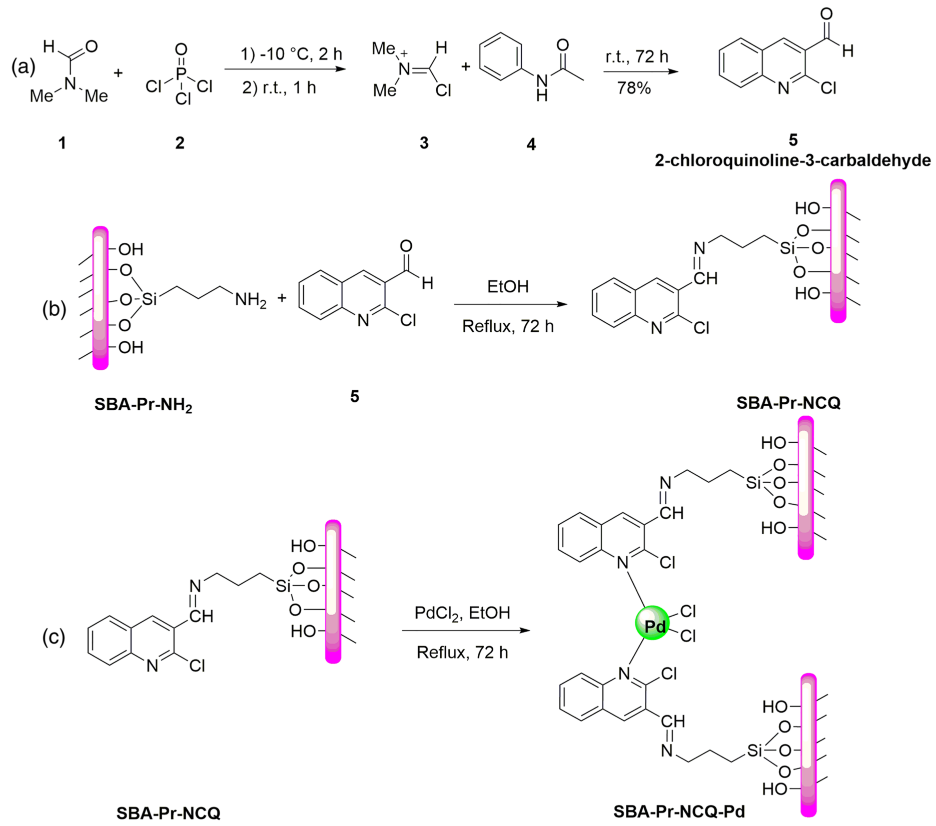

SCHEME 1 Synthetic procedure for the preparation of SBA-Pr-NCQ-Pd catalyst

acetanilide **4** to give 2-chloroquinoline-3-carbaldehyde **5** (CQC) (Scheme 1a). SBA-15 and SBA-Pr-NH_2 were prepared according to the literature.[47] In the following, SBA-Pr-NH_2 was functionalized with 2-chloroquinoline-3-carbaldehyde **5** in EtOH to afford SBA-Pr-NCQ via the formation of a C=N bond between the organic and inorganic parts (Scheme 1b). Finally, the SBA-Pr-NCQ-Pd nanocatalyst was obtained from the reaction of SBA-Pr-NCQ with $PdCl_2$ (Scheme 1c).

To characterize the catalyst, and to confirm the immobilization of Pd, Fourier Transform Infrared Spectroscopy (FT-IR) spectroscopy was used. The FT-IR spectra for SBA-15, SBA-Pr-NH_2, SBA-Pr-NCQ, and SBA-Pr-NCQ-Pd are shown in Figure 1. Two major bands at around 800–1,100 cm^{-1} are present in all spectra and are related to Si–O–Si stretching vibrations. In spectrum b, the peaks at 2878 and 2,937 cm^{-1} are characteristic of aliphatic $-CH_2$ groups, which confirms the successful introduction of propylamine groups onto the pore walls of SBA-15. The absence of the characteristic peaks of $-NH_2$ groups in spectrum b, which were expected to appear around 3,300–3,600 cm^{-1}, is assigned to the overlapping by the strong stretching band of OH groups of SBA-15. In spectrum c, there are four new peaks at 1648, 1498, 1,458 and 671 cm^{-1} as well as the bands already seen in spectrum b. The band at 1648 cm^{-1} is due to the imine bond formed from the reaction of propylamine groups on the surface of SBA-Pr-NH_2 with

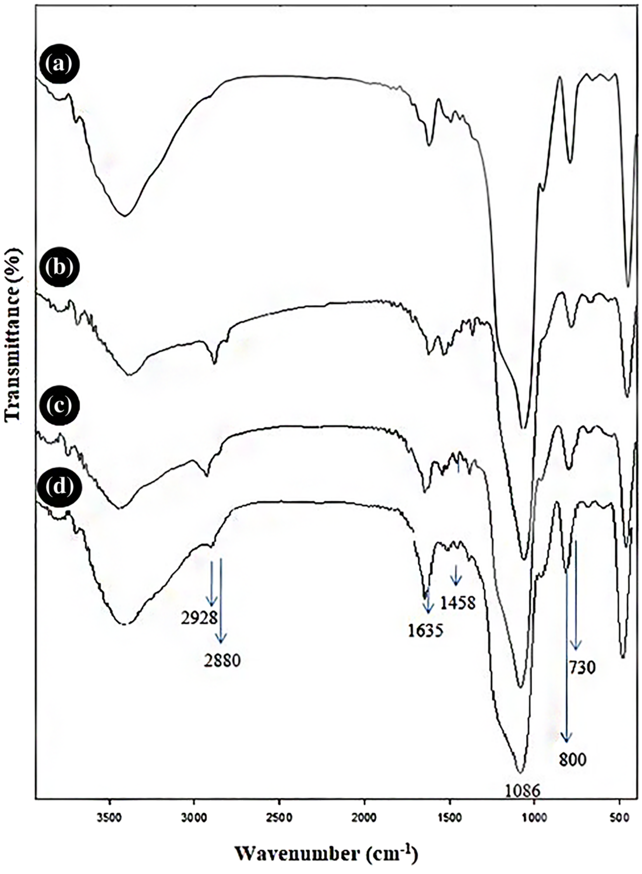

FIGURE 1 FT-IR spectra of (a) SBA-15, (b) SBA-Pr-NH_2, (c) SBA-Pr-NCQ, and (d) SBA-Pr-NCQ-Pd

2-chloroquinoline-3-carbaldehyde units. The peaks for C=C stretching vibrations of the aromatic ring can be seen at 1498 and 1,458 cm^{-1}. The C–Cl stretching vibrations appear at 671 cm^{-1}. Moreover, the band at 573 cm^{-1} in the spectrum of SBA-Pr-NCQ-Pd can be assigned to the stretching vibration of Pd–N.[48] These results provide evidence that the SBA-15 sample was successfully functionalized with Pd species to provide the final catalyst SBA-Pr-NCQ-Pd.

The low-angle X-Ray Diffraction (XRD) patterns of SBA-15, SBA-Pr-NCQ, and SBA-Pr-NCQ-Pd are shown in Figure 2. There are three well-resolved reflections for SBA-Pr-NCQ and SBA-Pr-NCQ-Pd such as SBA-15, which shows that the functionalized samples possess mesoordered hexagonal structures. For mesoporous SBA-15, three peaks are indexed to the (100), (110), and (200) reflections of the two-dimensional hexagonal space group *p6mm*. Figure 2 shows the lowering of reflection intensities in SBA-Pr-NCQ and SBA-Pr-NCQPd, which are due to the incorporation of organic compounds into the pore walls causing a partial lowering of the crystallinity, but the mesoporous structure has not been destroyed. Figure 3 shows the Scanning Electron Microscope (SEM) images of SBA-15, SBA-Pr-NCQ, and SBA-Pr-NCQPd, and demonstrates the preservation of uniformly sized

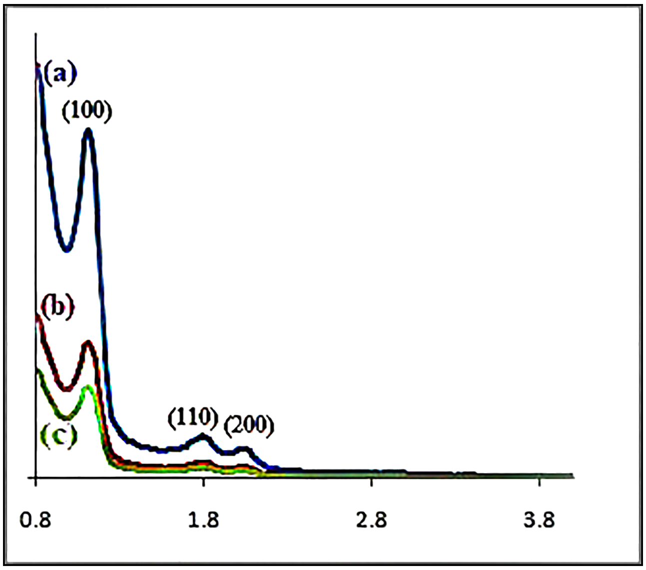

FIGURE 2 Low-angle powder XRD patterns of (a) SBA-15, (b) SBA-Pr-NCQ, and (c) SBA-Pr-NCQ-Pd

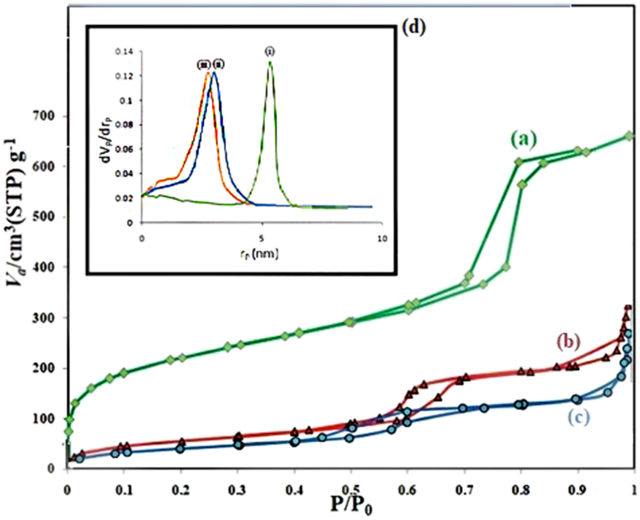

Sample	$^aS_{BET}$ (m^{2}g^{-1})	^{a}V (cm^{3}g^{-1})	$^aD_{BJH}$ (nm)
SBA-15	898	0.9	5.9
SBA-Pr-NCQ	144	0.25	3.14
SBA-Pr-NCQ-Pd	95	0.12	3.05

$^aS_{BET}$ is specific surface area, V total pore volume, and D_{BJH} average pore diameter

FIGURE 4 N2 adsorption–desorption isotherms of (a) SBA-15, (b) SBA-Pr-NCQ and (c) SBA-Pr-NCQ-Pd and pore size distributions of (d-i) SBA-15, (d-ii) SBA-Pr-NCQ and (d-iii) SBA-Pr-NCQ-Pd

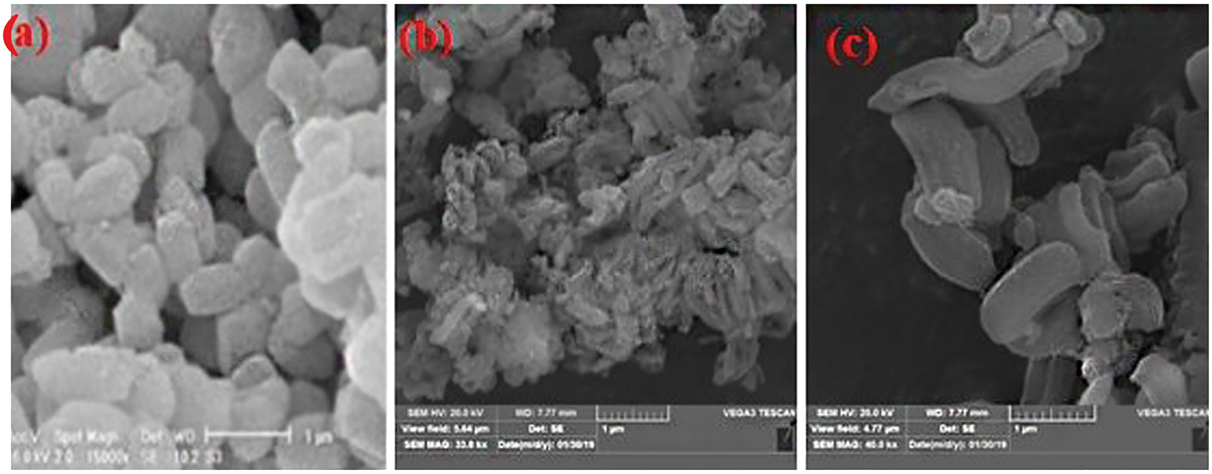

FIGURE 3 SEM images of (a) SBA-15, (b) SBA-Pr-NCQ, and (c) SBA-Pr-NCQ-Pd

pores after surface modification. The EDX spectrum of SBA-Pr-NCQ-Pd displays the elements, counting C (2.63%), N (4.00%), O (45.06%), Si (35.68%) and Pd (12.63%), which are present in the structure of this catalyst. The palladium peak confirms the immobilized Pd nanoparticles on the surface of SBA-Pr-NCQ.

The nitrogen adsorption–desorption isotherms and the BJH pore size distribution (based on the adsorption branch of the isotherms) for SBA-15, SBA-Pr-NH_2, SBA-Pr-NCQ, and SBA-Pr-NCQ-Pd are shown in Figure 4. The isotherms were characterized by the type IV with a H1-type hysteresis loop defined by IUPAC indicating that the surface area in SBA-Pr-NCQ-Pd was decreased. These results also show the three structural parameters of the samples: the specific surface area (Brunauer–Emmett–Teller method), the total pore volume, and the pore diameter (BJH method). Successful incorporation of functional organic materials into mesoporous SBA-15 silica pores and the inclusion of Pd in this structure shifted the pore size to a smaller value and led to a reduction in pore volume and surface area.

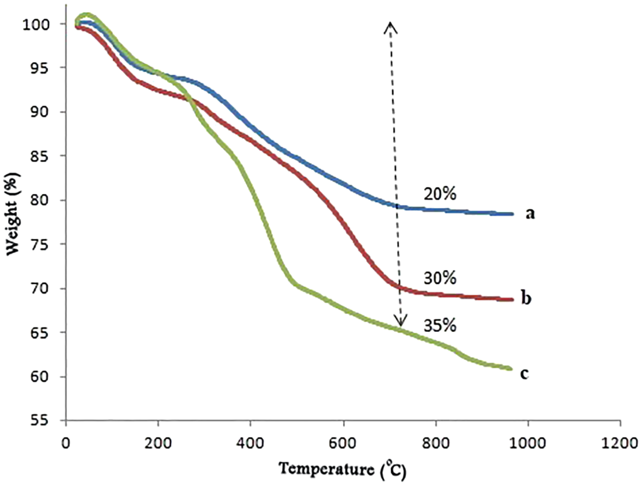

FIGURE 5 TGA curves of (a) SBA-Pr-NH_2, (b) SBA-Pr-NCQ, and (c) SBA-Pr-NCQ-Pd

The thermal stability of the functionalized SBA (SBA-Pr-NH_2, SBA-Pr-NCQ, and SBA-Pr-NCQ-Pd) was determined by Thermal Gravimetric Analysis (TGA), which presents the initial weight loss below 200 °C (Figure 5) and it can be attributed to the desorption of physically adsorbed water. The obvious mass change (30% and 35%) from 200 to 790°C is probably due to the decomposition of organic groups. The TGA curves therefore confirm the successful grafting of organic groups onto the surface of silica.

3.2 | Coupling reaction

To investigate the possible catalytic properties of SBA-Pr-NCQ-Pd in C–C bond formation (coupling reaction), the Mizoroki–Heck reaction was carried out. Various chemical parameters, such as solvent (ethanol, water, and toluene), base (K_2CO_3, NaOH, and Et_3N), amount of base, and catalyst, were studied to determine the best conditions. To optimize the reaction conditions, the Mizoroki–Heck coupling reaction of 4-iodobenzene and

TABLE 1 Different conditions used in the Mizoroki–Heck coupling reaction

No.	Catalyst (mol%)	Solvent	Base	Time (hr)	Yield (%)
1	0.15	H_2O	K_2CO_3 (1 mmol)	24	25
2	0.25	H_2O:EtOH (3:2)	K_2CO_3 (1 mmol)	24	43
3	0.04	H_2O:EtOH (3:2)	K_2CO_3 (1 mmol)	24	39
4	**0.25**	**H_2O:EtOH (3:2)**	**K_2CO_3 (2 mmol)**	**20 min**	**96**
5	0.25	H_2O	K_2CO_3 (2 mmol)	2	87
6	0.25	Toluene	K_2CO_3 (2 mmol)	24	20
7	0,25	H_2O:EtOH (3:2)	Et_3N (2 mmol)	24	20
8	0.25	H_2O:EtOH (3:2)	NaOH (2 mmol)	24	60

These data are optimized. Our best conditions demonstrated with bold values.

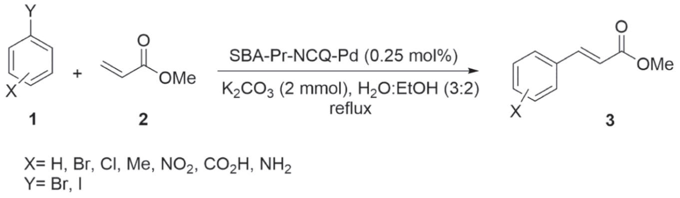

SCHEME 2 Mizoroki–Heck coupling reaction of aryl halides and methacrylate in the presence of SBA-Pr-NCQ-Pd catalyst

TABLE 2 Mizoroki–Heck coupling of aryl halides and methacrylate using SBA-Pr-NCQ-Pd as catalyst

No.	X	Y	Time (min)	Yield (%)	TON[a]	TOF (hr^{-1})[b]
1	4-NO_2	1-Br	35	98	819	1,412
2	2-NH_2	1-Br	40	93	693	1,051
3	4-Cl	1-Br	35	88	768	1,324
4	3-Me	1-Br	25	94	661	1,588
5	4-Me	1-Br	20	96	675	2027
6	4-Br	1-Br	15	91	877	3,508
7	H	I	20	96	1,105	3,317
8	2-CO_2H	1-I	40	90	741	1,112

[a] Turnover number, calculated as moles of product/moles of active sites.
[b] Turnover frequency, calculated as TON/time.

methacrylate was selected as the reaction model. As shown in Table 1, the best result was obtained when the reaction was carried out in the presence of 3 mg of SBA-Pr-NCQ in H_2O:EtOH (3:2) as solvent using K_2CO_3 (2 mmol) as the base at 70°C. With these optimized conditions, the Mizoroki–Heck reaction was investigated using several starting materials to give the desired products in high yield (Scheme 2 and Table 2). It is evident that 1,4-dibromobenzene reacted faster than other aryl halides (entry 6) in the reaction of aryl chlorides, and a low yield of product was obtained because of the strength of the C–Cl bond (entry 3). On the other hand, aryl halides with an electron drawing group reacted with methacrylate in longer reaction times (entries 1 and 8). Also, 4-methylbenzene versus 3-methylbenzene reacted with better reaction time and yield (entries 3 and 4). In the case of iodobenzene and bromobenzene, the corresponding products were obtained with high turnover frequencies (TOFs) of 3,508 and 3,317 h^{-1} (entries 6 and 7).

After the optimal conditions had been determined, the repeatability of this reaction using styrene and various derivatives of aryl halides was studied in the presence of SBA-Pr-NCQ-Pd catalysts (Scheme 3). As demonstrated in Table 3, stilbene derivatives were prepared in good to high yields. All IR and GC Mass of Heck products were provided in supporting information (Figures S6-S32).

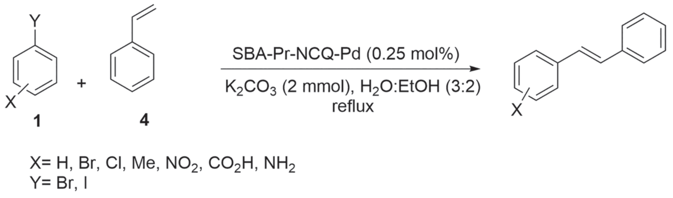

SCHEME 3 Mizoroki–Heck coupling reaction of aryl halides and styrene in the presence of SBA-Pr-NCQ-Pd catalyst

TABLE 3 Mizoroki–Heck coupling of aryl halides and styrene using SBA-Pr-NCQ-Pd as catalyst

No.	X	Y	Time (min)	Yield (%)	TON[a]	TOF (hr^{-1})[b]
00	4-NO_2	1-Br	70	87	783	671
11	2-NH_2	1-Br	90	82	640	426
12	4-Cl	1-Br	60	91	782	782
13	3-Me	1-Br	50	92	714	856
44	4-Me	1-Br	55	94	729	795
15	4-Br	1-Br	40	89	919	1,377
16	H	I	50	90	1,101	1,321
17	2-CO_2H	1-I	60	85	761	761

[a] Turnover number, calculated as moles of product/moles of active sites.
[b] Turnover frequency, calculated as TON/time.

3.3 | Catalyst leaching and recyclability

3.3.1 | Hot filtration test

A hot filtration test was performed for leaching of Pd from the catalyst during the Mizoroki-Heck reaction model under optimized conditions. For this purpose, after 10 min, the hot reaction mixture was filtered to separate off the catalyst and the reaction was continued under the same conditions with the supernatant solution. No increase in the product was observed (determined using GC–MS measurements) and no Pd was detected in the filtered solution by Inductively coupled plasma atomic emission spectroscopy (ICP-AES). This result proves that the Pd NPs are firmly grafted on the SBA-Pr-NCQ due to the excellent affinity between Pd NPs and 2-chloroquinoline-3-carbaldehyde ligand.

TABLE 4 Recycling study of SBA-Pr-NCQ-Pd

Run	1	2	3	4
Yield (%)	96	95	94	92

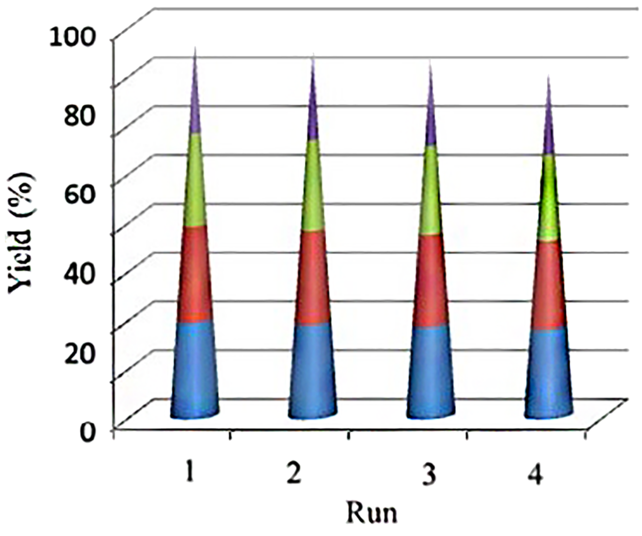

FIGURE 6 Recycling study of SBA--Pr-NCQ-Pd

3.3.2 | Reusability of catalyst

Recycling of the SBA-Pr-NCQ-Pd catalyst was carried out for the Mizoroki–Heck reaction of 4-iodobenzene and methacrylate under optimized reaction conditions. After the completion of each cycle, the Pd catalyst was filtered off from the reaction mixture, washed with hot solvents (ethyl acetate and ethanol), and dried under vacuum overnight then reused in a subsequent run. According to the results in Table 4 and Figure 6, the catalyst was highly reusable under the reaction conditions, preserving its initial catalytic performance almost unaltered after four uses. The ICP analysis determined the 3.5 and 3.2 wt% results for fresh and reused Pd catalyst.

To show the potential of our catalyst for the Heck reaction of aromatic aryl halides with methacrylate, the advantages of the present procedure were compared with those previously reported in the literature (Table 5). According to Table 5, SBA-Pr-NCQ-Pd catalyst showed a higher performance than some of the other reported catalysts used in Heck reaction in terms of shorter reaction times, higher stability, high TOF, and better reaction yields.

TABLE 5 Results of this work compared with some recently reported procedures[a]

No.	Catalyst	Temperature (°C)	Time (hr)	Yield (%)	TOF (hr^{-1})
1	SBA-15-Pd	140	3	97	2,500[1,39]
2	SBA-15-Pd	140	2	88	–[2,49]
3	SBA-15-Pd	120	2	88	–[3,50]
4	SBA-15-TAT-Pd(II)	120	1	95	–[4,51]
5	$PdCl_2$	120	5	75	–[5,52]
6	SBA-R/Im-NH_2.Pd	90	40 min	98	–[6,53]
7	Pd@OMP-IL-Bn	100	0.5	99	20,000[54]
8	SWCNT-PAMAM3.0-Pd	90	5	99	–[8,55]
9	POSS	120	5	99	476[56]
10	$Ti_{0.97}Pd_{0.03}O_{1.97}$	110	4	98	159[57]
11	**SBA-Pr-NCQ-Pd**	**70**	**20 min**	**96 (this work)**	**3,317**

These data are optimized. Our best conditions demonstrated with bold values.

[a] The conditions were compared for the reaction of 4-iodobenzene with methacrylate

4 | CONCLUSION

In summary, the present study reports the functionalization of SBA-15-NH_2 with 2-chloroquinoline-3-carbaldehyde to form SBA-Pr-NCQ and a post-modification process with palladium ions to form a highly stable and recyclable catalyst SBA-Pr-NCQ-Pd nanoreactor as a heterogeneous catalyst for the Mizoroki–Heck coupling reaction of aryl halides and methacrylate in mixed EtOH–H_2O solvent under mild reaction conditions. The SBA-Pr-NCQ-Pd catalyst could be easily separated by filtration and reused at least four times without a significant decrease in catalytic activity.

ACKNOWLEDGMENTS

We gratefully acknowledge financial support from the Research Council of Alzahra University and the University of Tehran.

ORCID

Razieh Moradi https://orcid.org/0000-0002-6271-0142
Ghodsi Mohammadi Ziarani https://orcid.org/0000-0001-5177-7889
Alireza Badiei https://orcid.org/0000-0002-6985-7497
Fatemeh Mohajer https://orcid.org/0000-0003-0587-2230

REFERENCES

[1] S. Lee, C. Jo, R. Ryoo, *J. Mater. Chem. A* **2017**, *5*, 11086.
[2] D. A. Gomez-Gualdron, S. T. Dix, R. B. Getman, R. Q. Snurr, *Physic. Chem. Chem. Physic.* **2015**, *17*, 27596.
[3] P. Serp, E. Castillejos, *Chem. Cat. Chem.* **2010**, *2*, 41.
[4] C. Deraedt, L. Salmon, D. Astruc, *Adv. Synth. Catal.* **2014**, *356*, 2525.
[5] G. Mohammadi Ziarani, N. Lashgari, A. Badiei, *Curr. Org. Chem.* **2017**, *21*, 674.
[6] V. F. Vavsari, G. Mohammadi Ziarani, S. Balalaie, A. Latifi, M. Karimi, A. Badiei, *Tetrahedron* **2016**, *72*, 5420.
[7] J. Afshani, A. Badiei, N. Lashgari, G. Mohammadi Ziarani, *RSC Adv.* **2016**, *6*, 5957.
[8] N. Lashgari, A. Badiei, G. Mohammadi Ziarani, F. Faridbod, *Anal. Bioanal. Chem.* **2017**, *409*, 3175.
[9] M. Karimi, A. Badiei, G. Mohammadi Ziarani, *RSC Adv.* **2015**, *5*, 36530.
[10] I. K. Mbaraka, D. R. Radu, V. S.-Y. Lin, B. H. Shanks, *J. Catal.* **2003**, *219*, 329.
[11] V. Zeleňák, M. Badaničová, D. Halamova, J. Čejka, A. Zukal, N. Murafa, G. Goerigk, *Chem. Eng. J.* **2008**, *144*, 336.
[12] J. Fan, C. Yu, J. Lei, Q. Zhang, T. Li, B. Tu, W. Zhou, D. Zhao, *J. Am. Chem. Soc.* **2005**, *127*, 10794.
[13] A. M. Chong, X. Zhao, A. T. Kustedjo, S. Qiao, *Microporous Mesoporous Mater.* **2004**, *72*, 33.
[14] A. Walcarius, M. Etienne, B. Lebeau, *Chem. Mater.* **2003**, *15*, 2161.
[15] X. Zhang, H. Dong, Z. Gu, G. Wang, Y. Zuo, Y. Wang, L. Cui, *Chem. Eng. J.* **2015**, *269*, 94.
[16] S. Fujita, S. Inagaki, *Chem. Mater.* **2008**, *20*, 891.
[17] W. Wang, J. E. Lofgreen, G. A. Ozin, *Small* **2010**, *6*, 2634.
[18] R. F. Heck, *J. Am. Chem. Soc.* **1969**, *91*, 6707.
[19] Y. Fujiwara, I. Moritani, S. Danno, R. Asano, S. Teranishi, *J. Am. Chem. Soc.* **1969**, *91*, 7166.
[20] A. M. Trzeciak, J. J. Ziółkowski, *Coordin. Chem. Rev.* **2007**, *251*, 1281.
[21] A. Biffis, M. Zecca, M. Basato, *J. Mol. Catal. A: Chem.* **2001**, *173*, 249.
[22] T. Mizutani, S. Honzawa, S. Tosaki, M. Shibasaki, *Angew. Chem., Int. Ed* 200, *2*(41), 4680.
[23] L. F. Tietze, G. Kettschau, U. Heuschert, G. Nordmann, *Chem. – Eur. J.* **2001**, *7*, 368.
[24] A. Häberli, C. J. Leumann, *Org. Lett.* **2001**, *3*, 489.
[25] C. Amatore, B. Godin, A. Jutand, F. Lemaitre, *Chem. – Eur. J.* **2007**, *13*, 2002.
[26] A. F. Littke, G. C. Fu, *J. Am. Chem. Soc.* **2001**, *123*, 6989.
[27] S. S. Pröckl, W. Kleist, M. A. Gruber, K. Köhler, *Angew. Chem. Int. Ed.* **2004**, *43*, 1881.
[28] F. Zhao, M. Shirai, Y. Ikushima, M. Arai, *J. Mol. Catal. A: Chem.* **2002**, *180*, 211.
[29] Z. Zhang, Z. Wang, *J. Org. Chem.* **2006**, *71*, 7485.
[30] N. Panziera, P. Pertici, L. Barazzone, A. M. Caporusso, G. Vitulli, P. Salvadori, S. Borsacchi, M. Geppi, C. A. Veracini, G. Martra, *J. Catal.* **2007**, *246*, 351.
[31] A. Papp, G. Galbács, Á. Molnár, *Tetrahedron Lett.* **2005**, *46*, 7725.
[32] L. Huang, Z. Wang, T. Ang, J. Tan, P. Wong, *Catal. Lett.* **2006**, *112*, 219.
[33] N. Ren, Y.-H. Yang, Y.-H. Zhang, Q.-R. Wang, Y. Tang, *J. Catal.* **2007**, *246*, 215.
[34] C. Yang, H. Wustefeld, M. Kalwei, F. Schiith, *Stud. Surf. Sci. Catal.* Elsevier **2004**, *154*, 2574.
[35] M. Opanasenko, P. Štěpnička, J. Čejka, *RSC Adv.* **2014**, *4*, 65137.
[36] P. Sharma, A. Singh, *Catal. Sci. Technol.* **2014**, *4*, 2978.
[37] X. Ma, Y. Zhou, J. Zhang, A. Zhu, T. Jiang, B. Han, *Green Chem.* **2008**, *10*, 59.
[38] H. Veisi, D. Kordestani, A. R. Faraji, J. Porous, *Mater.* **2014**, *21*, 141.
[39] P. Han, X. Wang, X. Qiu, X. Ji, L. Gao, *J. Mol. Catal. A: Chem.* **2007**, *272*, 136.
[40] J. Zhang, G.-F. Zhao, Z. Popović, Y. Lu, Y. Liu, *Mater. Res. Bull.* **2010**, *45*, 1648.
[41] H. Yang, X. Han, G. Li, Y. Wang, *Green Chem.* **2009**, *11*, 1184.
[42] S. Rostamnia, T. Rahmani, *Appl. Organomet. Chem.* **2015**, *29*, 471.
[43] X. J. Feng, M. Yan, X. Zhang, M. Bao, *Chin. Chem. Lett.* **2011**, *22*, 643.
[44] Y. Jiang, Q. Gao, *J. Am. Chem. Soc.* **2006**, *128*, 716.
[45] S. Rohani, G. Mohammadi Ziarani, A. Badiei, A. Ziarati, M. Jafari, A. Shayesteh, *Appl. Organomet. Chem.* **2018**, *32*, e4397.
[46] A. Vilsmeier, A. Haack, *Ber. Dtsch. Chem. Ges.* **1927**, *60*, 119.
[47] D. Zhao, J. Feng, Q. Huo, N. Melosh, G. H. Fredrickson, B. F. Chmelka, G. D. Stucky, *Science* **1998**, 279.

[48] K. Mukhopadhyay, B. R. Sarkar, R. V. Chaudhari, *J. Am. Chem. Soc.* **2002**, *124*, 9692.

[49] L. Li, L.-X. Zhang, J.-L. Shi, J.-N. Yan, J. Liang, *Appl. Catal. A* **2005**, *283*, 85.

[50] P. Wang, Q. Lu, J. Li, *Mater. Res. Bull.* **2010**, *45*, 129.

[51] C. Singh, K. Jawade, P. Sharma, A. P. Singh, P. Kumar, *Catal. Commun.* **2015**, *69*, 11.

[52] Z. Zhang, Z. Zha, C. Gan, C. Pan, Y. Zhou, Z. Wang, M.-M. Zhou, *J. Org. Chem.* **2006**, *71*, 4339.

[53] M. J. Nasab, A. R. Kiasat, *RSC Adv.* **2016**, *6*, 81614.

[54] B. Karimi, M. R. Marefat, M. Hasannia, P. F. Akhavan, F. Mansouri, Z. Artelli, F. Mohammadi, H. Vali, *ChemCatChem* **2016**, *8*, 2508.

[55] F. Giacalone, V. Campisciano, C. Calabrese, V. La Parola, Z. Syrgiannis, M. Prato, M. Gruttadauria, *ACS Nano* **2016**, *10*, 4627.

[56] C. Calabrese, V. Campisciano, F. Siragusa, L. F. Liotta, C. Aprile, M. Gruttadauria, F. Giacalone, *Adv. Synth. Catal.* **2019**, *361*, 3758.

[57] S. K. Bhat, J. D. Prasad, M. Hegde, *J. Chem. Sci.* **2019**, *131*, 20.

SUPPORTING INFORMATION

Additional supporting information may be found online in the Supporting Information section at the end of this article.

How to cite this article: Moradi R, Mohammadi Ziarani G, Badiei A, Mohajer F. Synthesis and characterization of mesoporous organosilica supported palladium (SBA-Pr-NCQ-Pd) as an efficient nanocatalyst in the Mizoroki–Heck coupling reaction. *Appl Organomet Chem*. 2020; e5916. https://doi.org/10.1002/aoc.5916